The contribution of GABA to glutamate/glutamine cycling and energy metabolism in the rat cortex *in vivo*

Anant B. Patel*[†‡], Robin A. de Graaf*[‡§], Graeme F. Mason[‡¶], Douglas L. Rothman*[‡§], Robert G. Shulman*[‡], and Kevin L. Behar[†‡¶]

Departments of *Diagnostic Radiology, [¶]Psychiatry, and [§]Biomedical Engineering, and [‡]Magnetic Resonance Research Center, Yale University School of Medicine, New Haven, CT 06520

Contributed by Robert G. Shulman, March 2, 2005

Previous studies have shown that the glutamate/glutamine (Glu/Gln) neurotransmitter cycle and neuronal glucose oxidation are proportional (1:1), with increasing neuronal activity above isoelectricity. GABA, a product of Glu metabolism, is synthesized from astroglial Gln and contributes to total Glu/Gln neurotransmitter cycling, although the fraction contributed by GABA is unknown. In the present study, we used ^{13}C NMR spectroscopy together with i.v. infusions of [1,6-$^{13}C_2$]glucose and [2-^{13}C]acetate to separately determine rates of Glu/Gln and GABA/Gln cycling and their respective tricarboxylic acid cycles in the rat cortex under conditions of halothane anesthesia and pentobarbital-induced isoelectricity. Under 1% halothane anesthesia, GABA/Gln cycle flux comprised 23% of total (Glu plus GABA) neurotransmitter cycling and 18% of total neuronal tricarboxylic acid cycle flux. In isoelectric cortex, glucose oxidation was reduced >3-fold in glutamatergic and GABAergic neurons, and neurotransmitter cycling was below detection. Hence, in both cell types, the primary energetic costs are associated with neurotransmission, which increase together as cortical activity is increased. The contribution of GABAergic neurons and inhibition to cortical energy metabolism has broad implications for the interpretation of functional imaging signals.

GABAergic neurons | glutamatergic neurons | magnetic resonance spectroscopy | neuronal–glial interactions

Glutamate (Glu) and GABA are the major excitatory and inhibitory neurotransmitters in the mature cerebral cortex and together account for ≈90% of total cortical synapses (1). Excitatory synapses outnumber inhibitory synapses ≈5:1 (2), suggesting that excitation plays an energetically dominant role in the cortex. The energetic cost of GABAergic neurotransmission remains an open question, however, because current methods used to assess cortical activity are based on changes in local blood flow or metabolism (e.g., glucose or oxygen consumption), which cannot differentiate glutamatergic from GABAergic neurons. Thus, the interpretation of changes in cortical activity in terms of the energetics of excitation and inhibition requires other methods that are sensitive to the synthesis of these neurotransmitters.

Glutamatergic neurotransmitter cycling flux and energy consumption have been reported for rat and human cortex by using ^{13}C NMR spectroscopy during the i.v. infusion of ^{13}C-labeled glucose (3–10). These studies show that the Glu/glutamine (Gln) cycling flux (V_{cyc}) is substantial, from ≈30% to 42% of neuronal tricarboxylic acid (TCA) cycle flux in anesthetized rats (V_{TCAn}) (4, 5, 8) to ≈38–50% of V_{TCAn} in resting awake rat and human cortex (7, 9, 10). In the cortex of anesthetized rats, changes in V_{cyc} and V_{TCAn} are proportional (≈1:1) over a large cortical activity range above isoelectricity (4, 8).

The determination of V_{cyc} from Gln and Glu ^{13}C turnover, using [1-^{13}C]glucose as tracer, includes contributions from GABA as well as Glu (4, 5, 11). This is because Gln is a common precursor, and ^{13}C labeling of Gln-C4 during GABA catabolism in glia is indistinguishable from direct labeling by neuronal Glu-C4 in the Glu/Gln cycle (Fig. 1). Thus, the contribution of glial GABA catabolism to Gln labeling and V_{cyc} has not been distinguished previously. The contribution of GABAergic neurons to energetics is particularly important because of recurring suggestions from neuroimaging studies, which are responsive to energy consumption, that inhibitory processes may require either no energy or very little energy (12).

In this study, we evaluated the contributions of GABAergic and glutamatergic neurotransmitter fluxes and their respective rates of glucose oxidation using ^{13}C and ^{1}H-[^{13}C]NMR spectroscopy during i.v. infusions of either [1,6-$^{13}C_2$]glucose or [2-^{13}C]-acetate. Whereas glucose is oxidized in both neurons and glia, acetate is metabolized almost exclusively in glia (13–16), providing a highly specific means of tagging the common glial Gln precursor of Glu and GABA. The steady-state fractional enrichments of Glu-C4, GABA-C2, and Gln-C4 attained during the infusion of [2-^{13}C]acetate were used to compute the ratios V_{cyc}/V_{TCAn} for glutamatergic and GABAergic neurons. The ratios were then used as parameter constraints in fitting a three-compartment metabolic model to the time courses of ^{13}C labeling of amino acids from [1,6-$^{13}C_2$]glucose, yielding values of the absolute neurotransmitter and TCA cycle fluxes for each neuronal cell type.

We found that, compared with glutamatergic neurons, GABAergic neurons consume a sizable but smaller fraction of total energy and contribute a similar fraction to the total (Glu plus GABA) neurotransmitter flux. Furthermore, both glutamatergic and GABAergic neurotransmitter cycling and energy consumption increased with neuronal activity above an isoelectric baseline. Our findings lend *in vivo* support to recent electrophysiological studies *in vitro* of proportional (balanced) changes in excitatory and inhibitory ion conductance with increasing activity (17).

Materials and Methods

Animal Preparation. All experiments were performed under protocols approved by the Yale Animal Care and Use Committee. Male Sprague–Dawley rats, fasted overnight, were anesthetized with halothane (2%), tracheotomized, and ventilated on 68% N_2O/30% O_2. The left femoral artery and both femoral veins were cannulated for the continuous monitoring of arterial blood pressure and blood gases and for the i.v. infusion of glucose and acetate, respectively. After surgery, halothane was reduced to ≈1% (Group A) or was discontinued and anesthesia maintained with pentobarbital (Group B). Core temperature was main-

Abbreviations: V_{cyc}, cycle flux; TCA, tricarboxylic acid; GAD, Glu decarboxylase; CMR, cerebral metabolic rate; α-KG, α-ketoglutarate.

[†]To whom correspondence may be addressed. E-mail: anant.patel@yale.edu or kevin.behar@yale.edu.

© 2005 by The National Academy of Sciences of the USA

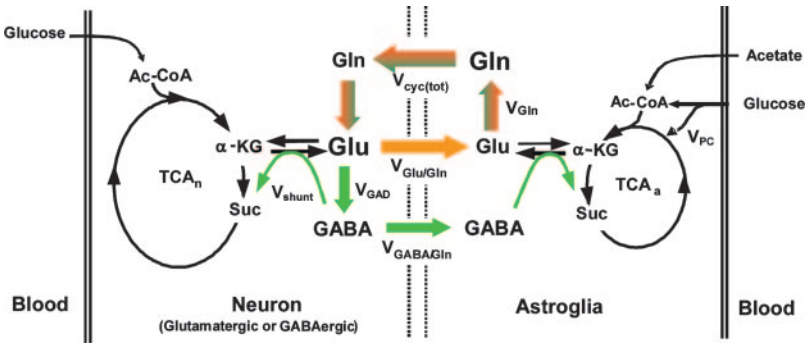

Fig. 1. Schematic depiction of Glu/Gln and GABA/Gln cycling between glutamatergic (orange) and GABAergic (green) neurons and astroglia relevant to ^{13}C NMR experiments using [1-^{13}C]glucose or [2-^{13}C]acetate as tracer. Metabolism of [1-^{13}C]glucose through glycolysis and the TCA cycle labels neuronal Glu-C4 and GABA-C2 with label transfer to Gln-C4 by neurotransmitter cycling, $V_{cyc(tot)} = V_{Glu/Gln} + V_{GABA/Gln}$. [2-^{13}C]acetate metabolism in astroglia labels Gln-C4 directly with label transfer to neuronal Glu-C4 and GABA-C2 by neurotransmitter cycling, $V_{cyc(tot)}$. V_{GAD}, rate of GABA synthesis via Glu decarboxylase; V_{shunt}, rate of neuronal GABA catabolism; V_{Gln}, rate of Gln synthesis; and V_{PC}, rate of pyruvate carboxylation.

tained near 37°C with a heating pad and a temperature-regulated recirculating water bath.

Animals in Group A (halothane anesthesia) were infused with either [1,6-$^{13}C_2$]glucose and unlabeled acetate (*in vivo* experiment) or [2-^{13}C]acetate and unlabeled glucose (*ex vivo* experiment). The glucose infusion followed the schedule described previously (18). Acetate was administered by bolus-variable rate infusion over 2 h (3 M dissolved in water, pH adjusted to 7.0) at 1.25 mmol/min per kg (0–5 min), 0.625 mmol/min per kg (5–10 min), and 0.25 mmol/min per kg thereafter. The 2-h infusion time was sufficient for Glu-C4, GABA-C2, and Gln-C4 to attain their steady-state ^{13}C enrichments. Additional bench experiments were conducted in which rats received [1,6-$^{13}C_2$]glucose and unlabeled acetate for 7 and 20 min to assess GABA ^{13}C turnover, which was too low in concentration to detect *in vivo* with sufficient sensitivity.

Animals in Group B (isoelectric) received sodium pentobarbital at a dose (120 mg/kg, i.p., with supplements of 10 mg/kg every 20 min) sufficient to induce and maintain isoelectricity as assessed by continuous electroencephalography (4). The rats in Group B received [1,6-$^{13}C_2$]glucose and acetate for 20 min using the same infusion protocol as described for Group A. No attempt was made to measure steady-state labeling from [2-^{13}C]acetate due to the very low metabolic rate. The high dose of pentobarbital (Group B) led to a decrease in mean arterial blood pressure to 50–60 mmHg (1 mmHg = 133 Pa).

Arterial blood gasses were maintained within normal physiological limits for rats in both groups. Arterial blood samples were taken periodically for the analysis of the concentration and ^{13}C enrichments of plasma glucose and acetate. After each experiment, the brain was immediately frozen *in situ* with liquid N_2 while mechanical ventilation was continued (19).

***In Vivo* NMR Spectroscopy.** *In vivo* NMR experiments were performed on a 7-T horizontal-bore NMR spectrometer/imager (Bruker AVANCE) operating at 75.50 MHz (^{13}C) and 300.30 MHz (^{1}H). ^{13}C NMR spectra were detected by using a circular surface coil of 14 mm diameter, whereas an outer butterfly coil was used for ^{1}H decoupling. Magnetic-field homogeneity was optimized by using FASTMAP (20). ^{1}H decoupled ^{13}C NMR spectra were obtained from a localized volume ($9 \times 4 \times 10$ mm^3) by using a polarization transfer pulse sequence in which the 90° and 180° pulses were replaced with adiabatic half- and full-passage pulses, respectively (9). Suppression of signals outside the localized volume was achieved by using outer volume suppression along the *x*, *y*, and *z* (axial) dimensions (21). ^{13}C NMR spectra were acquired every 1.5 sec in blocks of 128 scans (≈4 min per spectrum).

Analysis of Plasma Glucose and Acetate. The concentration of glucose in plasma samples was determined by using a Beckman Glucose Analyzer II (Beckman Coulter). The ^{13}C isotopic enrichment of plasma glucose and the concentration and ^{13}C enrichment of plasma acetate were determined from filtered (10-kDa) samples at 11.74 T by using ^{1}H NMR (Bruker AVANCE AM500). ^{1}H-[^{13}C]NMR spectra of plasma samples were also obtained at the conclusion of [2-^{13}C]acetate infusions to assess potential ^{13}C labeling in glucose.

Preparation of Tissue Extracts. Frozen tissue (150–200 mg) from frontoparietal cortex was ground with 0.1 M HCl/methanol (2:1 vol/wt) at −40°C followed by extraction with ice-cold ethanol (22). The supernatant was clarified by centrifugation, lyophilized, and resuspended in 500 μl of phosphate-buffered (100 mM, pH 7) D_2O (Cambridge Isotope Laboratories, Cambridge, MA) solution containing 3-trimethylsilyl[2,2,3,3-D_4]-propionate (0.5 mM). After the measurement of total amino acid concentrations in the extracts using ^{1}H-[^{13}C]NMR, the amino acids were separated by using AG1-X8 anion exchange chromatography, as described (22).

NMR Spectroscopy of Plasma and Brain Tissue Extracts. ^{1}H NMR spectra of plasma and brain extracts were acquired at 11.74 T (Bruker AVANCE AM500) under fully relaxed pulsing conditions. The ^{13}C enrichments of glucose-C1 (5.2 ppm) and acetate-C2 (1.9 ppm) in ^{1}H NMR spectra were calculated as the ratio of ^{13}C satellites to the total resonance intensity. ^{1}H-[^{13}C]NMR spectra of brain tissue extracts were acquired by using a pulse sequence incorporating adiabatic pulses for ^{1}H and ^{13}C excitation (23). The concentrations of metabolites were determined relative to [2-^{13}C]glycine added during tissue extraction. The isotopic ^{13}C enrichments of Glu (C4,C3), Gln (C4,C3), and GABA (C2,C3) in the separated fractions were determined as the ratio of ^{13}C-bound ^{1}H to total ^{1}H (^{12}C+^{13}C) for each carbon position.

Determination of the V_{cyc}/V_{TCA} During [2-^{13}C]Acetate Infusion. The differential equations that describe the flow of ^{13}C through the Glu/Gln and GABA/Gln cycles were solved analytically for the steady-state condition (see *Derivation of flux ratios* in *Supporting Text*, which is published as supporting information on the PNAS web site), which yielded the following relationships between V_{cyc} and V_{TCA} for glutamatergic (24) and GABAergic neurons:

$$V_{cyc(Glu/Gln)}/V_{TCA(Glu)} = Glu_{Glu4}/(Gln_{a4} - Glu_{Glu4}) \quad [1]$$

$$V_{cyc(GABA/Gln)}/V_{TCA(GABA)} = GABA_{GABA2}/(Gln_{a4} - GABA_{GABA2}), \quad [2]$$

where Glu_{Glu4}, $GABA_{GABA2}$, and Gln_{a4} represent the steady-state ^{13}C enrichments of amino acids during the infusion of [2-^{13}C]acetate and unlabeled glucose in the neuronal or astroglial (a) compartment. GABA and Gln were assumed to be entirely neuronal and glial, respectively, whereas Glu-C4 was corrected for glial Glu assuming the latter to be 10% of total Glu

with a steady-state ^{13}C enrichment given by Gln-C4. The ^{13}C enrichments were also corrected for the small amount of ^{13}C labeling that appeared in blood glucose-C1 during the [2-^{13}C]acetate infusion by subtraction of the ^{13}C enrichment of lactate-C3 (3.5 ± 0.3%), the latter assumed to reflect pyruvate-C3.

Metabolic Modeling of ^{13}C Time-Course Data. The metabolic fluxes were determined by fitting the three-compartment metabolic model [glutamatergic neuron, GABAergic neuron, and astroglia; (25)] depicted in Fig. 1 to the time courses of ^{13}C enrichments of Glu-C4, Glu-C3, and Gln-C4 measured *in vivo*, and Glu-C4, Glu-C3, GABA-C2, GABA-C3, Gln-C4, and Gln-C3 measured *ex vivo* during the [1,6-$^{13}C_2$]glucose and acetate infusions. The values of the ratios $V_{cyc(Glu/Gln)}/V_{TCA(Glu)}$ and $V_{cyc(GABA/Gln)}/V_{TCA(GABA)}$ (Eqs. **1** and **2**) were fixed as model constraints. Mass and ^{13}C isotope flows from [1,6-$^{13}C_2$]glucose into neuronal and glial Glu and Gln pools were written as coupled differential equations (see *Mass and isotope balance equations* in *Supporting Text*) within the CWAVE software package running in MATLAB (26). The equations were solved by using a first-/second-order Runge–Kutta algorithm, and fitting was done by using a Levenburg–Marquardt algorithm. Total Gln and GABA pools were assigned to the glial and GABAergic neuronal compartments, respectively, whereas Glu was divided between glutamatergic neurons (88%), glia (10%), and GABAergic neurons (2%) (27, 28). Pyruvate carboxylase flux (V_{PC}) was assumed to be 20% of the rate of total Gln synthesis (5, 29). Astroglial TCA cycle flux was assumed to be 15% of total TCA cycle flux (24). The cerebral metabolic fluxes were determined from the best fits of the model to the time-course data sets by using a simulated annealing algorithm (30). Cerebral metabolic rates of glucose oxidation [$CMR_{glc(ox)}$] were calculated as $\frac{1}{2}V_{TCA}$.

Determination of Cerebral Metabolic Fluxes During Pentobarbital-Induced Isoelectricity. For animals in Group B (isoelectric), the rates of glucose oxidation in glutamatergic and GABAergic neurons were calculated from the quantity of ^{13}C trapped in amino acids after a 20-min infusion of [1,6-$^{13}C_2$]glucose and acetate. Because of the slow rate of cerebral metabolism under these conditions, the rate of glucose oxidation in the two cell types was approximated from the initial rate of label accumulation in Glu and GABA according to:

$$CMR_{glc(Glu)} = (1/time)(1/Glc_1) \cdot\{(0.88[Glu])(Glu_4 + 2Glu_3) + 0.45[Asp](2Asp_3)\} \quad [3]$$

$$CMR_{glc(GABA)} = (1/time)(1/Glc_1) \cdot\{[GABA](GABA_2 + (2GABA_3)) + 0.45[Asp](2Asp_3)\}, \quad [4]$$

where [Glu], [GABA], and [Asp] are the total tissue concentrations; Glc_1 is the percent ^{13}C enrichment of plasma glucose-C1; and Glu_i, Asp_i, and $GABA_i$ are the percent ^{13}C enrichments at *i*th carbon. Tissue aspartate was assumed to be distributed between neurons (90%) and glia (10%), with equal percentages in glutamatergic (45%) and GABAergic (45%) neurons. Total neurotransmitter cycling [$V_{cyc(tot)}$] and V_{PC} were calculated by taking into account that Gln resulting from pyruvate carboxylase flux leads to equivalent contributions between Gln-(C3+C2) and Gln-C4, such that the excess labeling in Gln-C4 arises from neurotransmitter cycling with neuronal Glu-C4 as precursor.

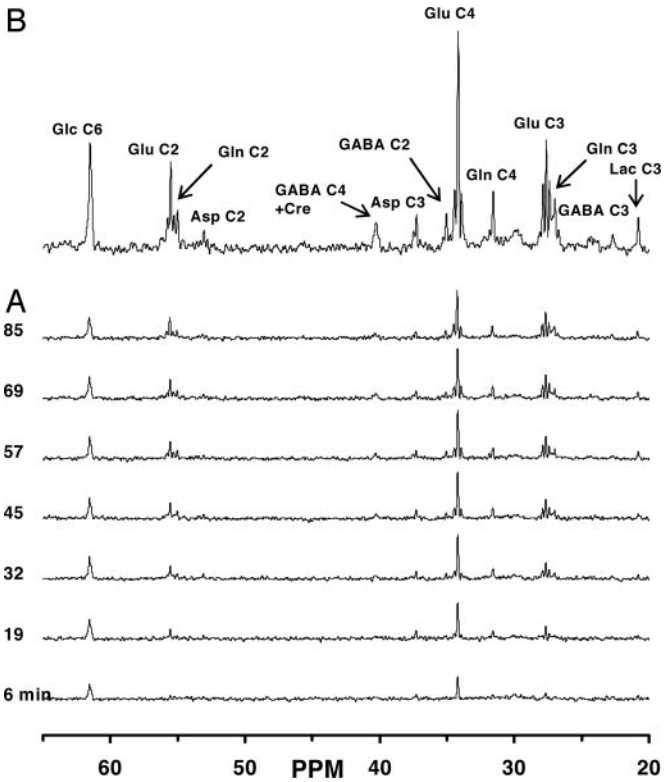

Fig. 2. Spatially localized ^{13}C-[^1H]NMR spectrum of metabolites in the intact rat brain after infusion of [1,6-$^{13}C_2$]glucose and acetate under halothane. Time courses of ^{13}C-labeling of metabolites (*A*) and averaged spectrum over the last 30 min (60–90 min) of the 1.5-h [1,6-$^{13}C_2$]glucose and acetate infusion (*B*). Peak label definitions: Asp, aspartate; Lac, lactate; Glc, glucose.

$$V_{cyc(tot)} = V_{cyc(Glu/Gln)} + V_{cyc(GABA/Gln)} = (1/time)(2/Glu_4)\{[Gln](Gln_4–(1.5Gln_3))\} \quad [5]$$

$$V_{PC} = (1/time)(1/Glc_1)([Gln](1.5Gln_3)), \quad [6]$$

where [Gln] and Gln_i are the Gln concentration and fractional enrichments, respectively. The factor of 1.5 arises from incomplete equilibration of OAA-C2 and OAA-C3 (5).

Results

Enrichment of Plasma Glucose and Acetate. The preinfusion concentrations of plasma glucose and acetate were similar in animals of both groups [Group A (halothane), glucose, 4.6 ± 0.9 mM, and acetate, 0.23 ± 0.10 mM; Group B (isoelectric), glucose, 5.2 ± 0.6 mM]. The infusion of [1,6-$^{13}C_2$]glucose and acetate increased plasma glucose concentrations and percentage enrichments to similar levels in both groups within minutes, and these values remained relatively constant thereafter (Group A, 9.5 ± 0.8 mM, 53 ± 2%; Group B, 12.6 ± 0.1 mM, 47 ± 5%). The infusion of [2-^{13}C]acetate/glucose in Group A increased plasma acetate concentration (15.8 ± 6.2 mM) and enrichments (>90%) to constant levels within the first 3–4 min of the infusion.

^{13}C Labeling of Cerebral Amino Acids During [1,6-$^{13}C_2$]Glucose and Acetate Infusion [Group A (Halothane)]. Fig. 2*A* depicts the time course of ^{13}C labeling of cortical amino acids in spatially localized ^1H-decoupled ^{13}C NMR spectra after infusion of [1,6-$^{13}C_2$]glucose and acetate *in vivo*. The ^{13}C spectrum (Fig. 2*B*) displays well resolved resonances and isotopomer splittings of Glu (C4, C3, and C2), Gln (C4, C3, and C2), GABA (C2, C3, and

Table 1. Cortical amino acid concentrations and percentage ^{13}C enrichments during [1,6-$^{13}C_2$]glucose/acetate and [2-^{13}C]acetate/glucose infusions in rats under halothane and pentobarbital (isoelectric) anesthesia

	Glu		Gln		GABA		Aspartate
	C4	C3	C4	C3	C2	C3	C3
Group A (halothane)							
Total concentration, μmol/g, $n = 11$	14.4 ± 1.3		6.8 ± 0.4		1.8 ± 0.5		4.3 ± 0.5
[1,6-$^{13}C_2$]Glucose/acetate, $\%E_{ep}$, $n = 12$	34.4 ± 1.0	24.5 ± 0.6	22.2 ± 1.8	17.3 ± 1.2	29.1 ± 1.1	13.3 ± 1.2	26.9 ± 4.5
[2-^{13}C]Acetate/glucose, $\%E_{ep}$, $n = 12$	10.9 ± 0.3	9.3 ± 0.9	23.4 ± 3.6	12.0 ± 1.5	11.1 ± 1.2	10.2 ± 2.0	6.6 ± 2.8
Group B (pentobarbital),							
Total concentration, μmol/g, $n = 4$	12.1 ± 1.5		8.3 ± 0.6		2.6 ± 0.2		3.1 ± 0.8
[1,6-$^{13}C_2$]Glucose/acetate, $\%E_{20}$, $n = 4$	14.1 ± 2.2	2.0 ± 0.5	1.6 ± 0.6	0.7 ± 0.4	9.0 ± 2.4	1.0 ± 0.7	7.3 ± 2.5

$\%E_{ep}$, percent ^{13}C enrichment at end of experiment; $\%E_{20}$, percent ^{13}C enrichment at 20 min of infusion. Values represent mean ± SD.

C4), aspartate (C3 and C2), and glucose C6 (C1 not shown). The concentrations and endpoint ^{13}C enrichments of the amino acids were determined in cortical extracts (Table 1), which allowed normalization and quantitation of the ^{13}C time courses.

GABAergic and Glutamatergic Fluxes Under Halothane Anesthesia. The steady-state ^{13}C enrichments of Glu-C4, Gln-C4, and GABA-C2 as measured in the [2-^{13}C]acetate/glucose experiment (Table 1) were used to compute the ratio of neurotransmitter cycling to TCA cycle flux (V_{cyc}/V_{TCA}) for glutamatergic and GABAergic neurons for animals in Group A (halothane). Using the values in Table 1 with Eqs. **1** and **2** gave V_{cyc}/V_{TCAn} of 0.63 ± 0.10 (GABAergic) and 0.45 ± 0.09 (glutamatergic). The difference of the ratios was statistically significant ($P < 0.001$, $n = 12$).

The values of V_{TCAn} and V_{cyc} for both GABAergic and glutamatergic neurons were determined by fitting the metabolic model (constrained by V_{cyc}/V_{TCAn}) to the ^{13}C enrichment time courses of Glu-C4, Glu-C3, GABA-C2, GABA-C3, and Gln-C4 measured *in vivo* during the [1,6-$^{13}C_2$]glucose and acetate infusion. The best fits of the metabolic model to the group-averaged time-course data are shown in Fig. 3 and best-fit parameter estimates in Fig. 4. Glucose oxidation in GABAergic and glutamatergic neurons was 18% and 82% of $CMR_{glc(tot)N}$, respectively (0.107 ± 0.012 vs. 0.495 ± 0.015 μmol/g per min), which includes both activity-dependent and independent contributions to the energetics. Neurotransmitter cycling in GABAergic and glutamatergic neurons was 23% and 77% of $V_{cyc(tot)}$, respectively (0.135 ± 0.015 vs. 0.445 ± 0.013 μmol/g per min), which was similar to their contribution to energy consumption.

Metabolic Fluxes in GABAergic and Glutamatergic Neurons During Isoelectricity. The cerebral metabolic fluxes for animals in Group B [pentobarbital (isoelectric)] were calculated from the rate of ^{13}C label accumulation into Glu, aspartate, GABA, and Gln during a 20-min [1,6-$^{13}C_2$]glucose and acetate infusion (Table 1

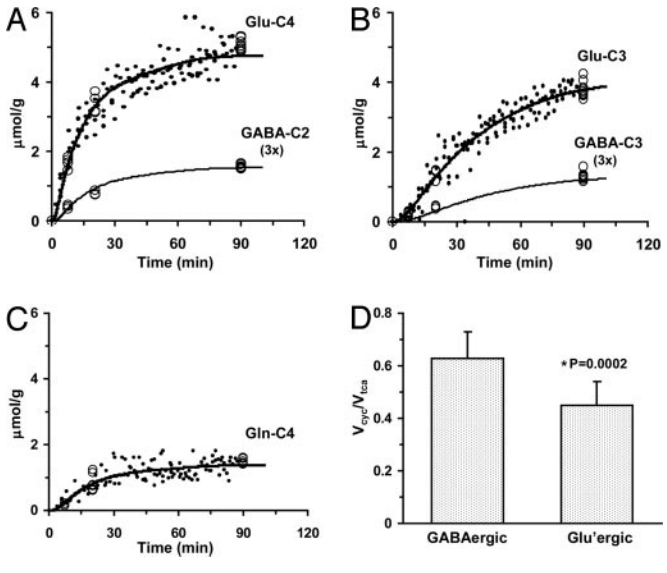

Fig. 3. Fit of the metabolic model to experimental data. The *in vivo* time course of ^{13}C labeling of Glu-C4 (*A*), Glu-C3 (*B*), and Gln-C4 (*C*) from [1,6-$^{13}C_2$]glucose is depicted for all animals (data points). *Ex vivo* measurements at selected time points are depicted by open circles in (*A*) Glu-C4 and GABA-C2, (*B*) Glu-C3 and GABA-C3, and (*C*) Gln-C4. The best fit of the mathematical model to the experimental data is shown by the smooth curves. (*D*) Values of the ratio, V_{cyc}/V_{TCA}, in glutamatergic and GABAergic neurons calculated from steady-state fractional enrichments of Glu-C4, Gln-C4, and GABA-C2 during infusion of [2-^{13}C]acetate and glucose (Table 1) used as constraints in the data fitting shown in *A–C*.

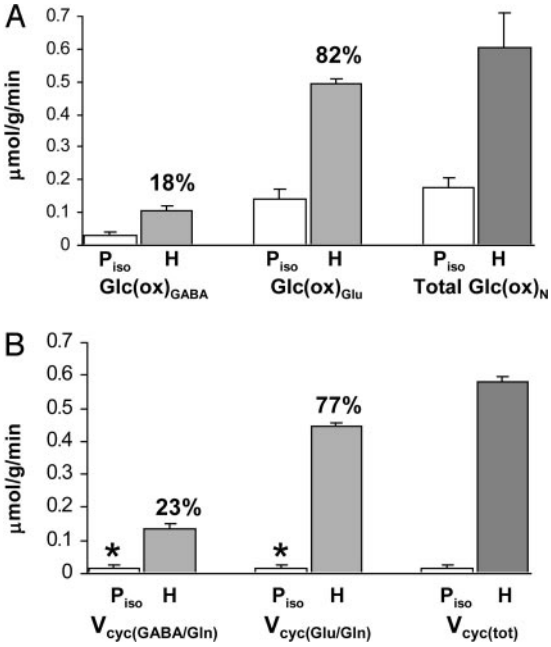

Fig. 4. Contribution of GABAergic and glutamatergic neurons to neuronal glucose oxidation and neurotransmitter cycling. (*A*) Rates of glucose oxidation, Glc(ox), for GABAergic and glutamatergic neurons and their sum, total $Glc(ox)_N$. (*B*) Rates of GABA/Gln and Glu/Gln cycling and their sum, $V_{cyc(tot)}$. P_{iso}, pentobarbital-induced isoelectricity; H, halothane/N_20 anesthesia. *, maximum possible value for P_{iso} condition given by the measured value of $V_{cyc(tot)}$ for isoelectricity. Percentages denote the contributions of GABAergic and glutamatergic neurons to the total fluxes given.

and Eqs. **3–6**). For the isoelectric cortex, $V_{cyc(tot)}$ was negligible (0.015 ± 0.013 μmol/g per min), as shown by the very low ^{13}C labeling of Gln-C4. Glucose oxidation in GABAergic neurons (0.030 ± 0.013 μmol/g per min) was ≈21% of that in glutamatergic neurons (0.143 ± 0.060 μmol/g per min) (Fig. 4). This finding is consistent with the 1:1 relationship for $\Delta V_{cyc(tot)}$ with $\Delta V_{TCAn(tot)}$ reported previously (4, 8). Comparison of the isoelectric (Group B) and more active halothane-anesthetized (Group A) animals showed that $V_{cyc(GABA/Gln)}$ and $V_{cyc(Glu/Gln)}$ had increased together with increased activity, as had their respective rates of glucose oxidation.

Discussion

Contribution of GABA to $V_{cyc(tot)}$ and Glial Energetics. Unlike Glu, which can undergo direct conversion to Gln in astroglia, catabolism of GABA is indirect, involving transamination with α-ketoglutarate (α-KG) (the only known acceptor of GABA nitrogen) to produce Glu and succinic semialdehyde, the latter being oxidized to succinate that enters the TCA cycle (31). The Glu formed by transamination can proceed to Gln (Fig. 1; see also Fig. 5, which is published as supporting information on the PNAS web site). However, glial oxidation of [1-^{13}C]glucose labels α-KG_{C4} and, through transamination with GABA, labels Glu_{C4} (and Gln_{C4}), rendering this pathway indistinguishable from glutamatergic cycling, $V_{cyc(Glu/Gln)}$. Thus, V_{cyc} as calculated from the labeling of Gln_{C4} in experiments using [1-^{13}C]glucose represents the sum of Glu and GABA cycling fluxes, i.e., $V_{cyc(tot)}$ (4, 5). Because transamination of GABA with α-KG requires a molar equivalent influx of acetylCoA, $V_{cyc(GABA/Gln)}$ can be viewed as a lower limit of this flux and the glial TCA semicycle from succinate to α-KG. Thus, for each molecule of GABA metabolized to α-KG through glial respiration, 11 molecules of ATP would be formed (3 $NADH_2$ = 9 ATP, 1 $FADH_2$ = 2 ATP), which is ≈92% (11/12) of the ATP expected from the complete oxidation of acetylCoA in the glial TCA cycle. Glial TCA cycle flux is estimated to be 15–25% of total oxidative metabolism (6, 24), suggesting that astroglial GABA catabolism could account for a substantial fraction of glial oxidative metabolism.

Comparison of $V_{cyc(GABA/Gln)}$ to Total GABA Synthesis. The rate of GABA synthesis catalyzed by Glu decarboxylase (GAD) in GABAergic neurons (V_{GAD}) at metabolic steady state (constant GABA level) must equal the sum of the catabolic fluxes in the GABA shunts of neurons and glia, given by V_{shunt} and $V_{cyc(GABA/Gln)}$, respectively (Fig. 1). Thus, $V_{cyc(GABA/Gln)} < V_{GAD}$. V_{GAD} can be estimated if the shunt flux in GABAergic neurons is known. In a ^{13}C NMR labeling study of mouse brain, Hassel *et al.* (32) reported that in GABAergic neurons, glucose oxidation in the pathway from α-KG to succinate is divided about equally between the TCA cycle and the GABA shunt. In our study, $V_{TCA(GABA)}$ sums all pathways from α-KG to succinate, which includes the GABA shunt in GABAergic neurons (25). Thus, an estimate of V_{GAD} using this information yields $V_{TCA(GABA)}/2 + V_{cyc(GABA/gln)} = 0.11 + 0.14 = 0.25$ μmol/g per min. Although this value is 1.3- to 2.0-fold higher than the range in V_{GAD} previously reported for rat cortex under α-chloralose anesthesia (25), energy metabolism was also ≈2× higher under halothane, which might explain this difference [$V_{TCAn(tot)}$ of 1.2 μmol/g per min vs. 0.5 μmol/g per min].

Neuronal Reuptake vs. Glial Clearance of Extracellular GABA. Astroglia play a dominant role in the clearance of Glu after synaptic release (33), but the clearance of GABA involves neuronal and glial transport (33–36), and both processes are highly regulated (35, 37). It is generally believed that GABA reuptake dominates clearance because of the higher density of GABA transporters in neurons than glia (33), although quantitative information on reuptake *in vivo* does not yet exist. Although the present findings relate only to GABA synthesis from Gln and not to reuptake per se, the results do provide an estimate of the maximum potential reuptake flux. If we assume that depolarization-related GABA release, which includes Ca^{2+}-dependent (exocytosis) and -independent (transporter reversal) release, is coupled to GABA synthesis (V_{GAD}), then an upper estimate of reuptake is given by the neuronal shunt flux, V_{shunt}, which is the difference between V_{GAD} and $V_{cyc(GABA/Gln)}$ (Figs. 1 and 5). As discussed above, V_{shunt} is comparable in magnitude to $V_{cyc(GABA/Gln)}$, so to the extent that GABA reuptake occurs, it will add to GABA release and thus influence extracellular levels and inhibition; however, the rate of steady-state GABA release should neither exceed V_{GAD} nor influence the measured value of cycling from glial Gln to GABAergic neurons, $V_{cyc(Gln/GABA)}$. Thus, $V_{cyc(Gln/GABA)}$ will underestimate the rate of GABA release to the extent GABA is cleared by reuptake, whereas both processes would be included in the measured value of $CMR_{glc(ox)}$, which includes all pathways of release coupled to GABA synthesis.

In the scheme depicted in Fig. 1, $V_{cyc(GABA/Gln)}$ returns Gln-derived carbon to the glia and therefore does not require anaplerosis (V_{PC}) to maintain this flux. On the other hand, to the extent that GABA synthesized from Gln did not return to glia, anaplerosis (V_{PC}) would be expected to balance this flow such that $V_{cyc(Gln/GABA)} = V_{cyc(GABA/Gln)} + V_{PC(GABA)}$. In either case, ^{13}C labeling of αKG_{C4} (and Gln_{C4}) would be the same, as would the value of $V_{cyc(Gln/GABA)}$. The only difference would be that $V_{cyc(Gln/GABA)}$ now contains a portion of flux arising from V_{PC}, as described for $V_{cyc(Glu/Gln)}$ (38). A recent study by Oz *et al.* (7) suggests that V_{PC} increases with total neuronal activity, supporting a role in neurotransmitter cycling. However, questions remain as to the total fraction of V_{PC} devoted to replacing lost Glu or GABA and dependence on activity. For example, the finding that V_{PC} did not increase acutely with $V_{cyc(tot)}$ during bicuculline seizures (29), which is known to increase GABAergic and glutamatergic activity (8, 39), suggests that V_{PC} may not be immediately responsive to large changes in neuronal activity.

Relationship of GABAergic Fluxes to Cortical Activity. $V_{cyc(tot)}$ in isoelectric cortex was only 3% of that under halothane and just 11% and <4% of $V_{cyc(GABA/Gln)}$ and $V_{cyc(Glu/Gln)}$, respectively. The low value of $V_{cyc(tot)}$ for isoelectric cortex (0.015 μmol/g per min) is consistent with findings in previous studies (4, 40) for the activity-independent or "housekeeping" oxidative metabolism of neurons. Thus, both neurotransmitter fluxes had increased with the higher state of cortical activity associated with halothane. Evidence that GABAergic inhibitory pathways are more active during increased activity has been reported. Persistent network activity *in vitro* is associated with increased spiking rates of both glutamatergic pyramidal neurons and fast-spiking GABAergic interneurons (17, 41). In ferret-brain slices, persistent recurrent activity, which is characteristic of anesthetized and certain sleep states, involves nearly balanced and proportional increases in both excitatory and inhibitory synaptic currents (17). A theoretical study using a cortical network model predicted a linear relationship between inhibitory and excitatory conductances, with slopes ranging from 1:1 to 1:5 (42). During seizures, the rate of GABA synthesis is substantially increased (39) when total glucose and oxygen consumption is increased (43), as well as $V_{cyc(tot)}$ and $CMR_{glc(ox)N}$ (8). Direct afferent stimulation of cerebellar inhibitory neurons has also been shown to increase cerebral blood flow (44), consistent with known mechanisms of energy metabolism and its coupling to hemodynamics.

Contribution of GABAergic Neurons to Cortical Oxidative Metabolism. In the neocortex, excitatory (glutamatergic) pyramidal neurons and inhibitory (GABAergic) interneurons are estimated to be 70–85% and 15–30% of total neurons (45, 46), respectively.

Inhibitory synapses account for ≈14–17% of total neocortical synapses (2). In the present study, GABAergic neurons accounted for 18% of neuronal oxidative metabolism (Fig. 4) or 13–15% of the total oxidative metabolism of neurons and glia, assuming that glia contributes 15–25% of total TCA cycle flux (6, 24). Remarkably, the relative fluxes appear similar to their relative synaptic densities. This value is near the range (15–25%) reported for the GABAergic TCA cycle flux based on cortical GABA-C2 turnover during [1-^{13}C]glucose infusion (25) but is substantially greater than estimates (1–2%) based on rates of cortical GABA synthesis after GABA-transaminase inhibition (47), which is likely to underestimate the absolute rate of GABA synthesis and its contribution to total oxidative metabolism. In whole brain of awake mice, GABAergic TCA cycle flux was reported to be ≈34% of total oxidation based on ^{13}C labeling of amino acids from [1-^{13}C]glucose and [2-^{13}C]acetate (32), although measurement of whole brain may emphasize higher GABAergic fluxes in subcortical structures (e.g., substantia nigra), and the cortex could be lower.

Implications of GABAergic Activity in Functional Neuroimaging. Neuronal activation in functional imaging studies is traditionally concerned with excitatory synapses (48, 49). The basic mechanisms coupling cellular activity to energy demand, however, are likely to be similar at excitatory and inhibitory synapses (50, 51). *In vivo* studies showing increased ^{14}C-2-deoxyglucose uptake in areas densely populated by inhibitory synapses during selective stimulation of inhibitory pathways are consistent with this idea (52, 53). In cerebellum, stimulation of inhibitory parallel fibers simultaneously with excitatory climbing fibers increases the total local field potential and cerebral blood flow (44, 54). Thus, reduced activity at excitatory synapses could arise directly from decreased afferent stimulation or by activation of GABAergic interneurons (55). Therefore, the interpretation of the functional neuroimaging signal in terms of excitation is limited by the unknown contribution of inhibitory and excitatory pathways to energy consumption. Waldvogel *et al.* (12) recently concluded that excitatory synaptic activity contributed to the blood oxygenation level dependent signal, whereas synaptic inhibition was less metabolically demanding than excitation. Although the present study shows that GABAergic activity contributes quantitatively less than glutamatergic activity, energy consumption increased in both cell types as activity increased, suggesting that GABAergic inhibition is of energetic importance during activation.

We thank Ms. Bei Wang for preparation of the animals, Terry Nixon and Scott McIntyre for NMR engineering support and maintenance, and Peter Brown for fabrication of the coils used in this study. This study was supported by National Institutes of Health Grants NS34813 and DK27121 (to K.L.B.), EB002097 (to R.A.d.G.), and AA-13430 (to G.F.M.) and a National Alliance for Research on Schizophrenia and Depression Young Investigator Award (to K.L.B.).

1. Peters, A. & Jones, E. G. (1984) *Cerebral Cortex: Cellular Components of the Cerebral Cortex* (Plenum, New York).
2. Beaulieu, C. & Colonnier, M. (1985) *J. Comp. Neurol.* **231,** 180–189.
3. Sibson, N. R., Dhankhar, A., Mason, G. F., Behar, K. L., Rothman, D. L. & Shulman, R. G. (1997) *Proc. Natl. Acad. Sci. USA* **94,** 2699–2704.
4. Sibson, N. R., Dhankhar, A., Mason, G. F., Rothman, D. L., Behar, K. L. & Shulman, R. G. (1998) *Proc. Natl. Acad. Sci. USA* **95,** 316–321.
5. Sibson, N. R., Mason, G. F., Shen, J., Cline, G. W., Herskovits, A. Z., Wall, J. E., Behar, K. L., Rothman, D. L. & Shulman, R. G. (2001) *J. Neurochem.* **76,** 975–989.
6. Gruetter, R., Seaquist, E. R. & Ugurbil, K. (2001) *Am. J. Physiol. Endocrinol. Metab.* **281,** E100–E112.
7. Oz, G., Berkich, D. A., Henry, P. G., Xu, Y., LaNoue, K., Hutson, S. M. & Gruetter, R. (2004) *J. Neurosci.* **24,** 11273–11279.
8. Patel, A. B., De Graaf, R. A., Mason, G. F., Kanamatsu, T., Rothman, D. L., Shulman, R. G. & Behar, K. L. (2004) *J. Cereb. Blood Flow Metab.* **24,** 972–985.
9. Shen, J., Petersen, K. F., Behar, K. L., Brown, P., Nixon, T. W., Mason, G. F., Petroff, O. A., Shulman, G. I., Shulman, R. G. & Rothman, D. L. (1999) *Proc. Natl. Acad. Sci. USA* **96,** 8235–8240.
10. Morris, P. & Bachelard, H. (2003) *NMR Biomed.* **16,** 303–312.
11. Behar, K. L. & Rothman, D. L. (2001) *J. Nutr.* **131,** 2498S–2504S.
12. Waldvogel, D., van Gelderen, P., Muellbacher, W., Ziemann, U., Immisch, I. & Hallett, M. (2000) *Nature* **406,** 995–998.
13. Badar-Goffer, R. S., Bachelard, H. S. & Morris, P. G. (1990) *Biochem. J.* **266,** 133–139.
14. Sonnewald, U., Westergaard, N., Hassel, B., Muller, T. B., Unsgard, G., Fonnum, F., Hertz, L., Schousboe, A. & Petersen, S. B. (1993) *Dev. Neurosci.* **15,** 351–358.
15. Sonnewald, U., Westergaard, N., Schousboe, A., Svendsen, J. S., Unsgard, G. & Petersen, S. B. (1993) *Neurochem. Int.* **22,** 19–29.
16. Waniewski, R. A. & Martin, D. L. (1998) *J. Neurosci.* **18,** 5225–5233.
17. Shu, Y., Hasenstaub, A. & McCormick, D. A. (2003) *Nature* **423,** 288–293.
18. Fitzpatrick, S. M., Hetherington, H. P., Behar, K. L. & Shulman, R. G. (1990) *J. Cereb. Blood Flow Metab.* **10,** 170–179.
19. Ponten, U., Ratcheson, R. A., Salford, L. G. & Siesjo, B. K. (1973) *J. Neurochem.* **21,** 1127–1138.
20. Gruetter, R. (1993) *Magn. Reson. Med.* **29,** 804–811.
21. Luo, Y., de Graaf, R. A., DelaBarre, L., Tannus, A. & Garwood, M. (2001) *Magn. Reson. Med.* **45,** 1095–1102.
22. Patel, A. B., Rothman, D. L., Cline, G. W. & Behar, K. L. (2001) *Brain Res.* **919,** 207–220.
23. de Graaf, R. A., Brown, P. B., Mason, G. F., Rothman, D. L. & Behar, K. L. (2003) *Magn. Reson. Med.* **49,** 37–46.
24. Lebon, V., Petersen, K. F., Cline, G. W., Shen, J., Mason, G. F., Dufour, S., Behar, K. L., Shulman, G. I. & Rothman, D. L. (2002) *J. Neurosci.* **22,** 1523–1531.
25. Mason, G. F., Martin, D. L., Martin, S. B., Manor, D., Sibson, N. R., Patel, A., Rothman, D. L. & Behar, K. L. (2001) *Brain Res.* **914,** 81–91.
26. Mason, G. F., Falk Petersen, K., de Graaf, R. A., Kanamatsu, T., Otsuki, T., Shulman, G. I. & Rothman, D. L. (2003) *Brain Res. Brain Res. Protoc.* **10,** 181–190.
27. Storm-Mathisen, J., Leknes, A. K., Bore, A. T., Vaaland, J. L., Edminson, P., Haug, F. M. & Ottersen, O. P. (1983) *Nature* **301,** 517–520.
28. Ottersen, O. P. & Storm-Mathisen, J. (1984) *J. Comp. Neurol.* **229,** 374–392.
29. Patel, A. B., Chowdhury, G. M. I., De Graaf, R. A., Rothman, D. L., Shulman, R. G. & Behar, K. L. (2005) *J. Neurosci. Res.* **79,** 128–138.
30. Press, W. H., Vetterling, W. T., Teukolsky, S. A. & Flannery, B. P. (1992) *Numerical Recipes in C: The Art of Scientific Computing* (Cambridge Univ. Press, New York).
31. Martin, D. L. & Tobin, A. J. (2000) in *GABA in the Nervous System: The View at Fifty Years*, eds. Martin, D. L. & Olsen, R. W. (Lippincott Williams & Wilkins, Philadelphia), pp. 25–41.
32. Hassel, B., Johannessen, C. U., Sonnewald, U. & Fonnum, F. (1998) *J. Neurochem.* **71,** 1511–1518.
33. Schousboe, A. (2003) *Neurochem. Res.* **28,** 347–352.
34. Conti, F., Minelli, A. & Melone, M. (2004) *Brain Res. Brain Res. Rev.* **45,** 196–212.
35. Barakat, L. & Bordey, A. (2002) *J. Neurophysiol.* **88,** 1407–1419.
36. Richerson, G. B. & Wu, Y. (2003) *J. Neurophysiol.* **90,** 1363–1374.
37. Beckman, M. L., Bernstein, E. M. & Quick, M. W. (1999) *J. Neurosci.* **19**, RC9.
38. Xu, Y., Oz, G., LaNoue, K. F., Keiger, C. J., Berkich, D. A., Gruetter, R. & Hutson, S. H. (2004) *J. Neurochem.* **90,** 1104–1116.
39. Chapman, A. G. & Evans, M. C. (1983) *J. Neurochem.* **41,** 886–889.
40. Choi, I. Y., Lei, H. & Gruetter, R. (2002) *J. Cereb. Blood Flow Metab.* **22,** 1343–1351.
41. Sanchez-Vives, M. V. & McCormick, D. A. (2000) *Nat. Neurosci.* **3,** 1027–1034.
42. Compte, A., Sanchez-Vives, M. V., McCormick, D. A. & Wang, X. J. (2003) *J. Neurophysiol.* **89,** 2707–2725.
43. Siesjo, B. K. (1978) *Brain Energy Metabolism* (Wiley, New York).
44. Caesar, K., Gold, L. & Lauritzen, M. (2003) *Proc. Natl. Acad. Sci. USA* **100,** 4239–4244.
45. Fairen, J. D. & Rogodor, J. (1994) in *Cerebral Cortex*, eds. Peters, A. & Jones, E. (Plenum, New York), pp. 201–253.
46. DeFelipe, J. & Farinas, I. (1992) *Prog. Neurobiol.* **39,** 563–607.
47. Martin, D. L. & Rimvall, K. (1993) *J. Neurochem.* **60,** 395–407.
48. Rothman, D. L., Behar, K. L., Hyder, F. & Shulman, R. G. (2003) *Annu. Rev. Physiol.* **65,** 401–427.
49. Bonvento, G., Sibson, N. & Pellerin, L. (2002) *Trends Neurosci.* **25,** 359–364.
50. Attwell, D. & Laughlin, S. B. (2001) *J. Cereb. Blood Flow Metab.* **21,** 1133–1145.
51. Jueptner, M. & Weiller, C. (1995) *NeuroImage* **2,** 148–156.
52. Nudo, R. J. & Masterton, R. B. (1986) *J. Comp. Neurol.* **245,** 553–565.
53. Ackermann, R. F., Finch, D. M., Babb, T. L. & Engel, J., Jr. (1984) *J. Neurosci.* **4,** 251–264.
54. Mathiesen, C., Caesar, K., Akgoren, N. & Lauritzen, M. (1998) *J. Physiol.* **512,** 555–566.
55. Lauritzen, M. (2001) *J. Cereb. Blood Flow Metab.* **21,** 1367–1383.